Journal of Molecular Catalysis A: Chemical 337 (2011) 77–81

Contents lists available at ScienceDirect

Journal of Molecular Catalysis A: Chemical

journal homepage: www.elsevier.com/locate/molcata

Gas-phase hydrogenation of maleic anhydride to γ-butyrolactone at atmospheric pressure over $Cu–CeO_2–Al_2O_3$ catalyst

Yang Yu, Yanglong Guo, Wangcheng Zhan, Yun Guo, Yanqin Wang, Yunsong Wang, Zhigang Zhang, Guanzhong Lu*

Key Laboratory for Advanced Materials, Research Institute of Industrial Catalysis, East China University of Science and Technology, Shanghai 200237, PR China

ARTICLE INFO

Article history:
Received 9 December 2010
Received in revised form 12 January 2011
Accepted 14 January 2011
Available online 27 January 2011

Keywords:
Maleic anhydride
γ-Butyrolactone
Gas-phase hydrogenation
$Cu–CeO_2–Al_2O_3$ catalyst
Deactivation

ABSTRACT

$Cu–CeO_2–Al_2O_3$ catalyst, prepared by co-precipitation method, was investigated for the gas-phase hydrogenation of maleic anhydride (MA) to γ-butyrolactone (GBL) at atmospheric pressure and the catalyst deactivation was also studied. Effects of catalyst composition, reaction temperature, and liquid hourly space velocity (LHSV) of raw material on the catalytic performance of $Cu–CeO_2–Al_2O_3$ catalyst were investigated. The catalyst (molar ratio of Cu:Ce:Al = 1:1:2) showed better catalytic performance, in which both the conversion of MA and the selectivity of GBL kept 100% within two hours under the reaction conditions of 6 mL catalyst, 0.1 MPa, 220–280 °C, 30 mL min^{-1} H_2, 0.6 h^{-1} LHSV of 20 wt.% MA/GBL. As for $Cu–CeO_2–Al_2O_3$ catalyst, smaller crystallite size of Cu and higher Cu surface area are favorable to increase its catalytic performance. The deactivation of $Cu–CeO_2–Al_2O_3$ catalyst is due to formation of the compact wax-like deposition on the catalyst surface, which is probably ascribed to the strong adsorption of succinic anhydride and then polymerization on the catalyst surface. The catalytic performance of the regenerated catalyst can be recovered completely by the regeneration method of N_2–air–H_2 stage treatment.

1. Introduction

γ-Butyrolactone (GBL) is an excellent organic solvent with high boiling point, and an important intermediate for production of N-methylpyrrolidone [1] and N-vinylpyrrolidone [2] based on its unique oxygen-contained five-membered ring structure. In addition, GBL is preferably used as the cell electrolyte instead of the strongly corrosion acid liquid [3,4].

GBL is produced by two main processes: dehydrogenation of 1,4-butanediol (BDO) [5] and hydrogenation of maleic anhydride (MA) [6,7]. The gas-phase catalytic hydrogenation of MA to GBL at atmospheric pressure has attracted increasing attention because of the simple process and the low-cost raw material of MA due to the large-scale industrialization and great improvement of the technology of oxidation of n-butane to MA. Many studies are concentrated on enhancing the conversion of MA and the selectivity of GBL, in which some catalysts has been reported, such as $Cu–ZnO–MgO–Cr_2O_3$ [8], $Cu–ZnO–Al_2O_3$ [9], $Cu–ZnO–TiO_2$ [10], Cu–Zn–Cd–Cr [11], $Cu–ZnO–CeO_2$ [12], $Cu–ZnO–ZrO_2$ [13], and $Cu–Pd(Ni)–TiO_2–Al_2O_3$ [14]. But there are still some disadvantages over those catalysts, such as higher reaction temperature, lower liquid hourly space velocity (LHSV) of raw material, higher H_2/MA molar ratio, lower selectivity of GBL, and poisonous composition of Cr in the catalyst.

As shown in Scheme 1, the catalytic hydrogenation of MA can produce several products, such as succinic anhydride (SA), GBL, tetrahydrofuran (THF), BDO and some hydrogenolysis products, such as propanol, propanoic acid, in which the selectivity of the target product is a principal criterion for catalyst screening. In this paper, $Cu–CeO_2–Al_2O_3$ catalyst, prepared by co-precipitation method, was investigated for the gas-phase hydrogenation of MA to GBL and the deactivation of the catalyst was also studied, which have not yet been reported.

2. Experimental

2.1. Preparation of $Cu–CeO_2–Al_2O_3$ catalyst

$Cu–CeO_2–Al_2O_3$ catalyst was prepared by co-precipitation method with 1.0 mol L^{-1} Na_2CO_3 aqueous solution as precipitating agent. 0.5 mol L^{-1} aqueous solution of $Cu(NO_3)_2·3H_2O$, $Ce(NO_3)_3·6H_2O$ and $Al(NO_3)_3·9H_2O$ with the given molar ratio, and the precipitating agent were added dropwise into 200 mL deionized water to keep pH value of the solution at 8–9 under vigorous stirring. The resultant precipitate was aged under gentle stirring at room temperature for 3 h and then washed by deionized water with

* Corresponding author. Tel.: +86 21 64252923; fax: +86 21 64252923.
E-mail addresses: ylguo@ecust.edu.cn (Y. Guo), gzhlu@ecust.edu.cn (G. Lu).

1381-1169/$ – see front matter © 2011 Elsevier B.V. All rights reserved.
doi:10.1016/j.molcata.2011.01.019

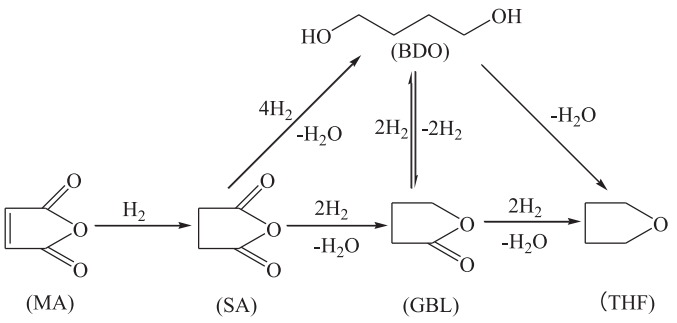

Scheme 1. The reaction pathway for catalytic hydrogenation of MA.

centrifugation until pH value of the filtrate was 7. After washed by ethanol for several times, the precipitate was dried at 120 °C overnight, and then calcined in air at 550 °C for 3 h and 650 °C for 3 h. The as-prepared catalyst was pressed and then crushed into 20–40 mesh particles for evaluation of its catalytic performance. The composition and physicochemical properties of Cu–CeO_2–Al_2O_3 catalysts were shown in Table 1.

2.2. Gas-phase hydrogenation of maleic anhydride

Gas-phase hydrogenation of maleic anhydride to γ-butyrolactone over Cu–CeO_2–Al_2O_3 catalyst was investigated in the quartz tubular fixed-bed reactor (inside diameter = 13 mm, length = 650 mm) at atmospheric pressure. In a bottom-up sequence, the reactor was packed with 1 mL quartz sand pretreated at 600 °C in air, 6 mL catalyst (height = 45 mm) and then 15 mL pretreated quartz sand for the complete gasification of raw material (MA dissolved in GBL, 20 wt.%). The catalyst was reduced in situ by 60 mL min^{-1} 5 vol.% H_2/N_2 at 380 °C for 7 h (designated as fresh catalyst). Then the temperature was lowered to 220 °C, 30 mL min^{-1} H_2 and LHSV of 0.6 h^{-1} of raw material were fed into the reactor. The products were collected in the conical beakers cooled by ice-bath at intervals of 1 h and analyzed by PerkinElmer Clarus 500 gas chromatograph equipped with a FID detector and a SE-54 capillary column (25 m × 0.32 mm × 1.0 μm). The temperatures of the injector and the detector were both 220 °C, and the temperature of the column oven was kept at 100 °C for 1 min and then increased programmedly from 100 °C to 120 °C at the rate of 5 °C min^{-1}.

2.3. Characterization of Cu–CeO_2–Al_2O_3 catalyst

The powder XRD patterns were recorded on a Bruker AXS D8 Focus diffractometer operated at 40 kV, 40 mA (Cu Kα radiation, λ = 0.15406 nm), and the diffraction patterns were taken in the range of $10° < 2\theta < 80°$ at the scanning rate of 6° min^{-1}.

The Cu surface area of Cu–CeO_2–Al_2O_3 catalyst was measured by N_2O chemisorption at 60 °C assuming a molar stoichiometry of Cu:N_2O = 2 and a surface atomic density of 1.46×10^{19} Cu atoms m^{-2} [15].

Table 1
The composition and physicochemical properties of Cu–CeO_2–Al_2O_3 catalysts.

Catalysts	Molar ratio			S_{BET} (m^2 g^{-1})	S_{Cu} (m^2 g^{-1})	Crystallite size of Cu (nm)
	Cu	Ce	Al			
C_{101}	1	0	1	80.1	19.6	12
C_{111}	1	1	1	65.6	8.9	20
C_{211}	2	1	1	50.3	8.0	27
C_{121}	1	2	1	83.7	12.8	26
C_{112}	1	1	2	107.8	18.7	15

The specific surface area was measured by nitrogen sorption at −196 °C with BET method on a NOVA 4200e surface area and pore size analyzer.

TG-DTA profiles were recorded on a PerkinElmer Pyris Diamond TG-DTA analyzers, in which the catalyst was heated programmedly from 40 °C to 800 °C at the rate of 10 °C min^{-1} in the atmosphere of air of 100 mL min^{-1}.

SEM images were recorded on a JEOL JSM-6360LV scanning electron microscope.

3. Results and discussion

3.1. Effect of catalyst composition

Table 2 shows the catalytic performance of Cu–CeO_2–Al_2O_3 catalyst for the gas-phase hydrogenation of MA to GBL at atmospheric pressure. Over CeO_2-free catalyst (C_{101}), the conversion of MA and the selectivity of GBL were only 70.4% and 64.7%, respectively, with the selectivity of SA of 21.5% and that of THF of 13.8% within the first hour. After reaction for 3 h, the conversion of MA and the selectivity of GBL dropped significantly to 50.7% and 50.8%, respectively. Compared with C_{101} catalyst, the catalytic performance was improved greatly with the introduction of CeO_2 into Cu–Al_2O_3 catalyst, in which the conversion of MA of 100% and the selectivity of GBL of 100% over C_{121} catalyst were achieved within the first hour. Compared with C_{111} catalyst, with an increase in Cu content in the catalyst, the corresponding catalytic performance dropped significantly and more SA was formed over C_{211} catalyst. With an increase in Al content in the catalyst, the catalytic performance was improved greatly over C_{112} catalyst, in which both the conversion of MA and the selectivity of GBL kept 100% within two hours. As for the gas-phase hydrogenation of MA to GBL [8], the multi-component products are easily formed and hence the design of a new catalyst should focus on suppressing overhydrogenation and hydrogenolysis of GBL. As shown in Table 2, except for a small quantity of overhydrogenation product (THF), no hydrogenolysis products were detected over Cu–CeO_2–Al_2O_3 catalysts. Therefore Cu–CeO_2–Al_2O_3 catalyst is very suitable for the gas-phase hydrogenation of MA to GBL at atmospheric pressure, in which C_{112} catalyst shows better catalytic performance.

Table 2
Catalytic performance of Cu–CeO_2–Al_2O_3 catalysts for the gas-phase hydrogenation of MA to GBL at atmospheric pressure.[a]

Catalysts	Reaction time (h)	MA conversion (%)	Selectivity (%)		
			GBL	THF	SA
C_{101}	1	70.4	64.7	13.8	21.5
	2	66.8	60.4	9.9	29.7
	3	50.7	50.8	4.6	44.6
C_{111}	1	100.0	93.5	1.5	5.0
	2	98.1	90.7	–	9.3
	3	95.0	87.1	–	12.9
C_{211}	1	100.0	87.1	4.9	8.0
	2	90.4	80.7	3.2	16.1
	3	87.7	61.2	1.7	37.1
C_{121}	1	100.0	100.0	–	–
	2	99.7	95.4	4.0	0.6
	3	90.8	92.7	2.7	4.6
C_{112}	1	100.0	100.0	–	–
	2	100.0	100.0	–	–
	3	98.8	97.9	0.1	2.0

[a] Reaction conditions: 6 mL catalyst, 220 °C, 30 mL min^{-1} H_2, and 0.6 h^{-1} LHSV of MA in GBL.

Table 3
Effect of reaction temperature on the catalytic performance of C_{112} catalyst.[a]

Reaction temperature (°C)	Reaction time (h)	MA conversion (%)	Selectivity (%)		
			GBL	THF	SA
220	1	100.0	100.0	–	–
	2	100.0	100.0	–	–
	3	98.8	97.9	0.1	2.0
	4	89.7	92.6	0.1	7.3
240	1	100.0	100.0	–	–
	2	100.0	100.0	–	–
	3	99.6	99.3	0.3	0.4
	4	94.1	97.0	0.2	2.8
260	1	100.0	100.0	–	–
	2	100.0	100.0	–	–
	3	100.0	98.0	1.5	0.5
	4	95.2	93.3	1.0	5.7
280	1	100.0	100.0	–	–
	2	100.0	100.0	–	–
	3	100.0	95.6	3.0	1.4
	4	95.8	90.2	1.2	8.6

[a] Reaction conditions: 6 mL catalyst, 0.1 MPa, 30 mL min^{-1} H_2, and 0.6 h^{-1} LHSV of MA in GBL.

3.2. Effect of reaction temperature

Table 3 shows effect of reaction temperature on the catalytic performance of C_{112} catalyst at atmospheric pressure. Both the conversion of MA and the selectivity of GBL were 100% within two hours at 220–280 °C. With an increase in reaction temperature, the decrease in the conversion of MA with the time on stream was suppressed to some extent; however, the selectivity of GBL presented a parabola-like type change and reached a maximum at 240 °C. Therefore the optimum reaction temperature for the gas-phase hydrogenation of MA to GBL over C_{112} catalyst was 240 °C in terms of the yield of GBL.

3.3. Effect of LHSV of raw material

Table 4 shows effect of LHSV of raw material on the catalytic performance of C_{112} catalyst at atmospheric pressure. With an increase in LHSV of raw material, the catalytic performance and the stability of C_{112} catalyst became worse and the selectivity of SA increased, in which both the conversion of MA and the selectivity of GBL kept 100% for 7 h at LHSV of 0.2 h^{-1} and only for 2 h at LHSV of 0.6 h^{-1}. The increase in LHSV of raw material, which shortens the contact time of MA on the surface of the catalyst, increases the selectivity of SA and thus results in the rapid deactivation of the catalyst. Therefore lower LHSV of raw material is beneficial to increase the catalytic performance and the stability of C_{112} catalyst.

3.4. Comparison of catalytic performance of Cu-based catalysts

Cu-based catalyst is preferred for the gas-phase hydrogenation of MA to GBL, in which some reported catalysts were summarized in Table 5. As shown in Table 5, the yield of GBL can reach 100% over Cu–CeO_2–Al_2O_3 and Cu–Pd(Ni)–TiO_2–Al_2O_3 catalysts, which agrees well with the viewpoint of Herrmann and Emig [16] that the multistep hydrogenation of MA or SA is stopped at the stage of GBL and 1,4-butanediol is not formed over zinc-free Cu-based catalysts. Compared with the reported Cu-based catalysts, Cu–CeO_2–Al_2O_3 (C_{112}) catalyst without poisonous composition shows better performance, such as higher yield of GBL, lower reaction temperature and H_2/MA molar ratio, and higher LHSV of raw material.

3.5. Characterization of Cu–CeO_2–Al_2O_3 catalyst

3.5.1. XRD

Fig. 1 shows XRD patterns of the as-prepared Cu–CeO_2–Al_2O_3 catalysts. The characteristic diffraction peaks of CuO (PDF# 65-2309) and CeO_2 (PDF# 34-0394) can be identified in XRD patterns

Table 4
Effect of LHSV of raw material on the catalytic performance of C_{112} catalyst.[a]

Reaction time (h)	MA conversion (%)			Selectivity (%)								
				GBL			THF			SA		
	0.2 (h^{-1})	0.4 (h^{-1})	0.6 (h^{-1})	0.2 (h^{-1})	0.4 (h^{-1})	0.6 (h^{-1})	0.2 (h^{-1})	0.4 (h^{-1})	0.6 (h^{-1})	0.2 (h^{-1})	0.4 (h^{-1})	0.6 (h^{-1})
1	100.0	100.0	100.0	100.0	100.0	100.0	–	–	–	–	–	–
2	100.0	100.0	100.0	100.0	100.0	100.0	–	–	–	–	–	–
3	100.0	100.0	99.6	100.0	100.0	99.3	–	–	0.3	–	–	0.4
4	100.0	100.0	94.1	100.0	100.0	97.0	–	–	0.2	–	–	2.8
5	100.0	100.0	80.4	100.0	94.2	87.3	–	0.8	–	–	5.0	12.7
6	100.0	100.0	60.2	100.0	80.7	69.3	–	0.4	–	–	18.9	30.7
7	100.0	97.3	46.3	100.0	71.2	57.2	–	0.1	–	–	28.7	42.8
8	100.0	92.5	33.2	99.7	59.7	44.7	0.1	–	–	0.2	40.3	55.3
9	99.5	82.5	29.5	99.0	40.2	36.2	–	–	–	1.0	59.8	63.8
10	88.2	70.2	28.7	91.2	36.0	22.6	–	–	–	8.8	64.0	77.3

[a] Reaction conditions: 6 mL catalyst, 0.1 MPa, 240 °C, and 30 mL min^{-1} H_2.

Table 5
The catalytic performance of Cu-based catalysts for gas-phase hydrogenation of MA to GBL.

Catalysts	Reaction temperature (°C)	Reaction pressure (MPa)	SV of MA	Consecutive reaction time (h)	H_2/MA molar ratio	Maximum GBL yield (%)	References
Cu–ZnO–MgO–Cr_2O_3	245	0.1	0.084[a]	N/A	121	82.7	[8]
Cu–ZnO–Al_2O_3	275	0.1	0.644[a]	N/A	299	96.0	[9]
Cu–ZnO–TiO_2	265	0.1	0.017[b]	1	200	99.2	[10]
Cu–ZnO–CdO–Cr_2O_3	245	0.1	N/A	N/A	299	88.0	[11]
Cu–ZnO–CeO_2	235	1.0	0.020[b]	1	50	91.1	[12]
Cu–ZnO–ZrO_2	220	1.0	0.020[b]	1	50	85.0	[13]
Cu–Pd(Ni)–TiO_2–Al_2O_3	220	0.1	0.036[b]	1	32	100.0	[14]
Cu–CeO_2–Al_2O_3	220	0.1	0.171[a]/0.143[b]	2	9	100.0	Our work

[a] The mass of MA per hour passed through 1 g catalyst (h^{-1}).
[b] The mass of MA per hour passed through 1 mL catalyst (g h^{-1} mL^{-1}).

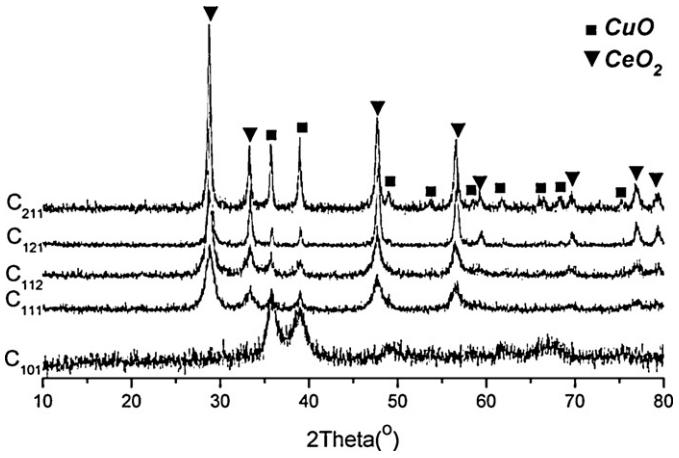

Fig. 1. XRD patterns of the as-prepared Cu–CeO_2–Al_2O_3 catalysts.

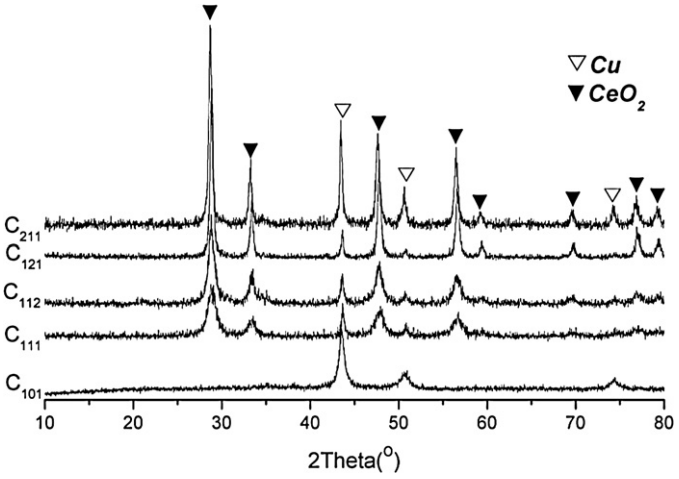

Fig. 2. XRD patterns of the fresh Cu–CeO_2–Al_2O_3 catalysts.

of all catalysts except for C_{101} catalyst, in which they located at $2\theta = 35.7^\circ$, 38.9°, 48.9°, 53.6°, 58.5°, 61.73°, 66.6°, 68.4°, 75.5° and 28.5°, 33.1°, 47.5°, 56.3°, 59.1°, 69.4°, 76.7°, 79.1°, respectively. Fig. 2 shows XRD patterns of the fresh Cu–CeO_2–Al_2O_3 catalysts. The characteristic diffraction peaks of CeO_2 remained, and the characteristic diffraction peaks of CuO disappeared, however the characteristic diffraction peaks of Cu (PDF# 65-9026) appeared at $2\theta = 43.3^\circ$, 50.5°, 74.2°, corresponding to the crystal planes of Cu (1 1 1), (2 0 0), (2 2 0), respectively. It indicated that CuO was reduced completely by 5 vol.% H_2/N_2 to Cu^0 and the state of CeO_2 did not change, in which Cu^0 is the active site for the gas-phase hydrogenation of MA to GBL [5,10,12,13]. The characteristic diffraction peaks of Al_2O_3 were not observed in Figs. 1 and 2, which indicated that Al_2O_3 existed in the amorphous phase in the catalysts.

The crystallite size of Cu was determined by Scherrer formula with the full peak width at half maximum height of the diffraction peak of Cu (1 1 1). Based on the diffraction peak of Cu (1 1 1) shown in Fig. 2, the crystallite size of Cu is shown in Table 1. As shown in Table 1, with the introduction of CeO_2 to Cu–Al_2O_3 catalyst or with an increase in Cu content in the catalyst, the crystallite size of Cu increased, however, with an increase in Al content in the catalyst, the crystallite size of Cu decreased. As for Cu–CeO_2–Al_2O_3 catalyst, smaller crystallite size of Cu is favorable to increase its catalytic performance.

3.5.2. Nitrogen sorption and N_2O chemisorption

The BET specific surface area (S_{BET}) and the Cu surface area (S_{cu}) of Cu–CeO_2–Al_2O_3 catalysts with different compositions were shown in Table 1. As shown in Tables 1 and 2, as for Cu–CeO_2–Al_2O_3 catalyst, the variation trend of its catalytic performance was fairly consistent with that of the corresponding S_{cu}, and higher S_{BET} was favorable to increase S_{cu}, that is to say, there were more active sites of Cu^0 on the catalyst surface, which resulted in better catalytic performance.

3.6. Deactivation and regeneration of Cu–CeO_2–Al_2O_3 catalyst

Cu–CeO_2–Al_2O_3 catalyst shows better catalytic performance for the gas-phase hydrogenation of MA to GBL at atmospheric pressure, but after reaction for several hours, the catalytic performance began to drop obviously. The similar phenomenon was also observed over Cu/SiO_2 catalyst [17]. To investigate the deactivation of Cu–CeO_2–Al_2O_3 catalyst, the fresh and the used C_{112} catalysts were characterized by SEM, TG-DTA and XRD. The used C_{112} catalyst was operated for 10 h under the reaction conditions of 6 mL catalyst, 0.1 MPa, 240 °C, 30 mL min^{-1} H_2, 0.6 h^{-1} LHSV of MA/GBL.

Fig. 3 shows SEM images of the fresh and the used C_{112} catalysts. As shown in Fig. 3, there were many small incompact particles on the surface of the fresh C_{112} catalyst. However, some compact wax-like surface deposition was present on the surface of the used C_{112} catalyst. As shown in Scheme 1, SA was a transition species in the catalytic hydrogenation of MA to GBL [6]. When

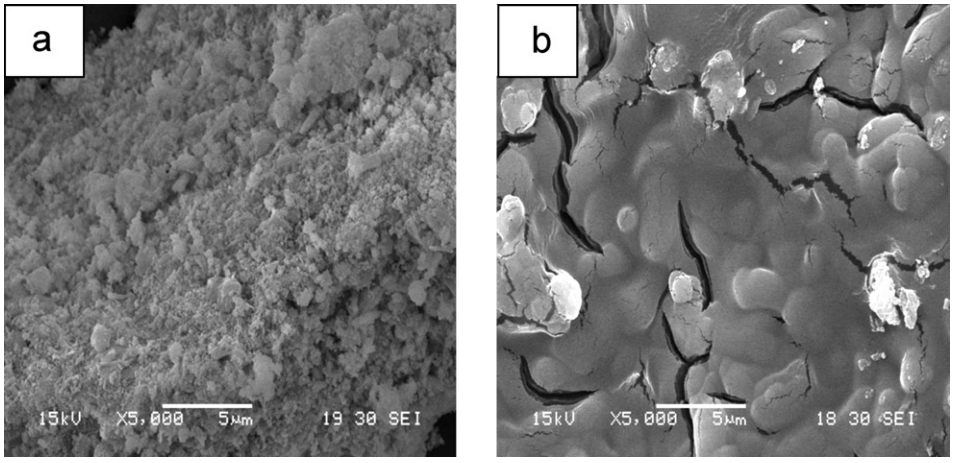

Fig. 3. SEM images of the as-prepared (a) and the used (b) C_{112} catalysts.

Table 6
The catalytic performance of the regenerated and the fresh C_{112} catalysts.[a]

Reaction time (h)	MA conversion (%)		Selectivity (%)					
	Fresh (*F*)	Regenerated (*R*)	GBL		THF		SA	
			F	*R*	*F*	*R*	*F*	*R*
1	100.0	100.0	100.0	100.0	–	–	–	–
2	100.0	100.0	100.0	100.0	–	–	–	–
3	99.6	99.0	99.3	98.6	0.3	0.1	0.4	1.3
4	94.1	94.3	97.0	96.7	0.2	-	2.8	3.3

[a] Reaction conditions: 6 mL catalyst, 0.1 MPa, 240 °C, 30 mL min^{-1} H_2, and 0.6 h^{-1} LHSV of MA in GBL.

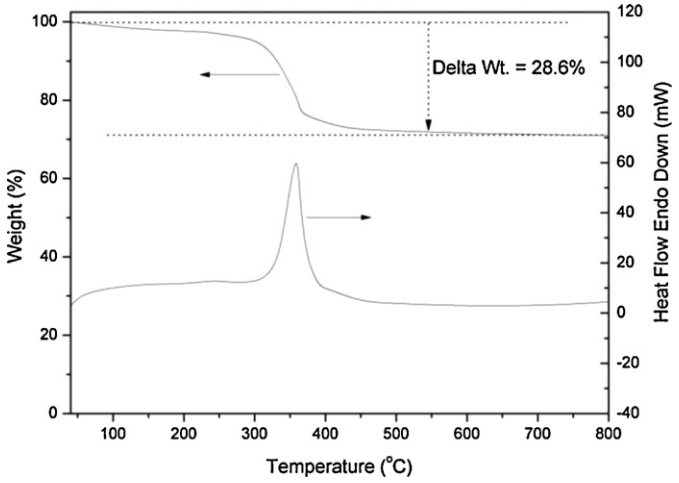

Fig. 4. TG-DTA profiles of the used C_{112} catalyst.

$Cu–CeO_2–Al_2O_3$ catalyst started to deactivate after reaction for several hours, both the conversion of MA and the selectivity of GBL decreased, and the selectivity of SA increased, that is to say, SA could not be hydrogenated to GBL promptly and was adsorbed strongly then polymerized on the catalyst surface, which resulted in the fast deactivation of catalyst.

Fig. 4 shows TG-DTA profiles of the use C_{112} catalyst. As shown in Fig. 4, the weight loss in the temperature range of 250–450 °C was 28.6% with an exothermic peak, which was ascribed to combustion of the surface depositions of the used C_{112} catalyst.

Based on TG-DTA analysis, the used C_{112} catalyst was regenerated in situ by the N_2–air–H_2 stage treatment, in which the used catalyst was purged by 50 mL min^{-1} N_2 at 200 °C for 1 h, then calcined in air at 450 °C for 4 h and finally reduced by 60 mL min^{-1} 5 vol.% H_2/N_2 at 380 °C for 4 h. The fresh and the regenerated C_{112} catalysts were characterized by XRD, in which there was no change in the characteristic diffraction peaks of Cu and CeO_2 and hence the active sites of Cu^0 did not change after regeneration. Table 6 shows the catalytic performance of the regenerated and the fresh C_{112} catalysts. As shown in Table 6, the catalytic performance of the regenerated C_{112} catalyst can be recovered completely.

4. Conclusions

Effects of catalyst composition, reaction temperature, and LHSV of raw material on the catalytic performance of $Cu–CeO_2–Al_2O_3$ catalyst for the gas-phase hydrogenation of MA to GBL at atmospheric pressure were investigated. C_{112} catalyst shows better catalytic performance, in which the conversion of MA and the selectivity of GBL were both 100% within two hours under the reaction conditions of 6 mL catalyst, 220–280 °C, 30 mL min^{-1} H_2, 0.6 h^{-1} LHSV of MA in GBL. Lower LHSV of raw material is beneficial to increase the catalytic performance and the stability of C_{112} catalyst. Smaller crystallite size of Cu and higher metallic Cu surface area are favorable to increase the catalytic performance of $Cu–CeO_2–Al_2O_3$ catalyst. The deactivation of $Cu–CeO_2–Al_2O_3$ catalyst is due to formation of the compact wax-like surface deposition of the catalyst, which is probably ascribed to the strong adsorption of SA and then polymerization on the surface of catalyst. The catalytic performance of the regenerated catalyst can be recovered completely by the regeneration method of N_2–air–H_2 stage treatment.

Acknowledgments

This project was supported financially by National Basic Research Program of China (2010CB732300) and Program for New Century Excellent Talents in University (NCET-09-0343).

References

[1] YS. Yoon, H.K. Shin, B.S. Kwak, Catal. Commun. 3 (2002) 349–355.
[2] Y. Shimasaki, H. Yano, H. Sugiura, H. Kambe, Bull. Chem. Soc. Jpn. 81 (2008) 449–459.
[3] J.Y. Huang, X.J. Liu, X.L. Kang, Z.X. Yu, T.T. Xu, W.H. Qiu, J. Power Sources 189 (2009) 458–461.
[4] S.S. Zhang, D. Foster, J. Read, J. Power Sources 188 (2009) 532–537.
[5] N. Ichikawa, S. Sato, R. Takahashi, T. Sodesawa, K. Inui, J. Mol. Catal. A: Chem. 212 (2004) 197–203.
[6] S.M. Jung, E. Godard, S.Y. Jung, K.C. Park, J.U. Choi, J. Mol. Catal. A: Chem. 198 (2003) 297–302.
[7] U.R. Pillai, E.S. Demessie, D. Young, Appl. Catal. B: Environ. 43 (2003) 131–138.
[8] M. Messori, A. Vaccari, J. Catal. 150 (1994) 177–185.
[9] G.L. Castiglioni, M. Ferrari, A. Guercio, A. Vaccari, R. Lancia, C. Fumagalli, Catal. Today 27 (1996) 181–186.
[10] T.J. Hu, H.B. Yin, R.C. Zhang, H.X. Wu, T.S. Jiang, Y.J. Wada, Catal. Commun. 8 (2007) 193–199.
[11] G.L. Castiglioni, A. Vaccari, G. Fierro, M. Inversi, M.L. Jacono, G. Minelli, I. Pettiti, P. Porta, M. Gazzano, Appl. Catal. A: Gen. 123 (1995) 123–144.
[12] D.Z. Zhang, H.B. Yin, R.C. Zhang, J.J. Xue, T.S. Jiang, Catal. Lett. 122 (2008) 176–182.
[13] D.Z. Zhang, H.B. Yin, C. Ge, J.J. Xue, T.S. Jiang, L.B. Yu, Y.T. Shen, J. Ind. Eng. Chem. 15 (2009) 537–543.
[14] W.J. Lu, G.Z. Lu, G.L. Lu, Y.L. Guo, J.S. Wang, Y. Guo, Chin. J. Catal. 23 (2002) 408–412.
[15] X.M. Guo, D.S. Mao, S. Wang, G.S. Wu, G.Z. Lu, Catal. Commun. 10 (2009) 1661–1664.
[16] U. Herrmann, G. Emig, Chem. Eng. Technol. 21 (1998) 285–295.
[17] C.I. Meyer, A.J. Marchi, A. Monzon, T.F. Garetto, Appl. Catal. A: Gen. 367 (2009) 122–129.